united nations
educational, scientific
and cultural
organization

international atomic
energy agency

the
abdus salam
international centre for theoretical physics

ICTP 40th Anniversary

SCHOOL ON SYNCHROTRON RADIATION AND APPLICATIONS
In memory of J.C. Fuggle & L. Fonda

19 April - 21 May 2004

Miramare - Trieste, Italy

1561/32

SAXS studies of proteins in solution

A. Craievich

SAXS studies of proteins in solution

SAXS studies of proteins in solution

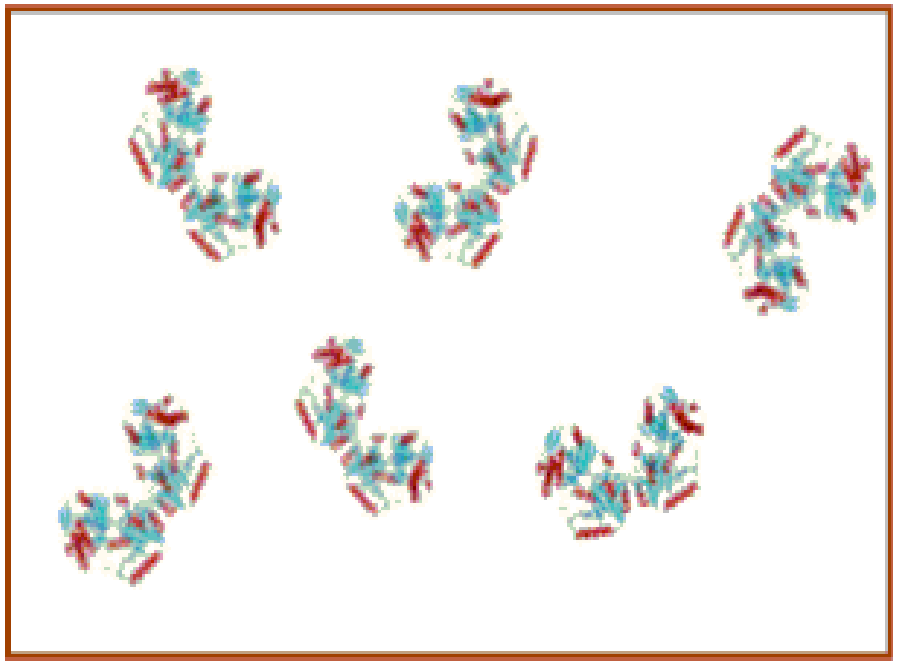

Protein single crystal

Assymetric unit

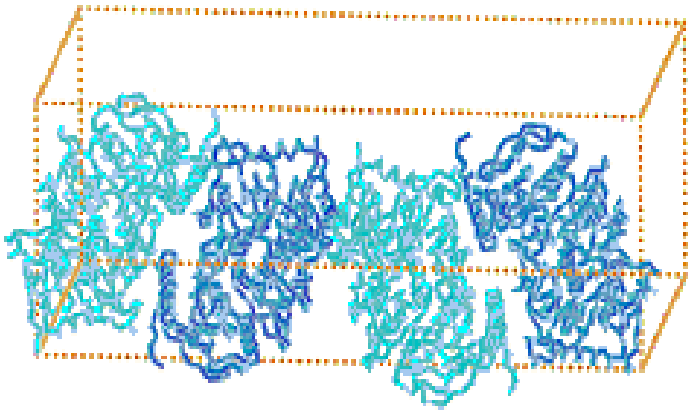

LNLS SAXS beamline

G. Kellermann, F. Vicentin, E. Tamura, M. Rocha, H. Tolentino, A. Barbosa, A. F. Craievich e I. L. C. Torriani, J. Appl. Cryst. (1997). 30, 880-883

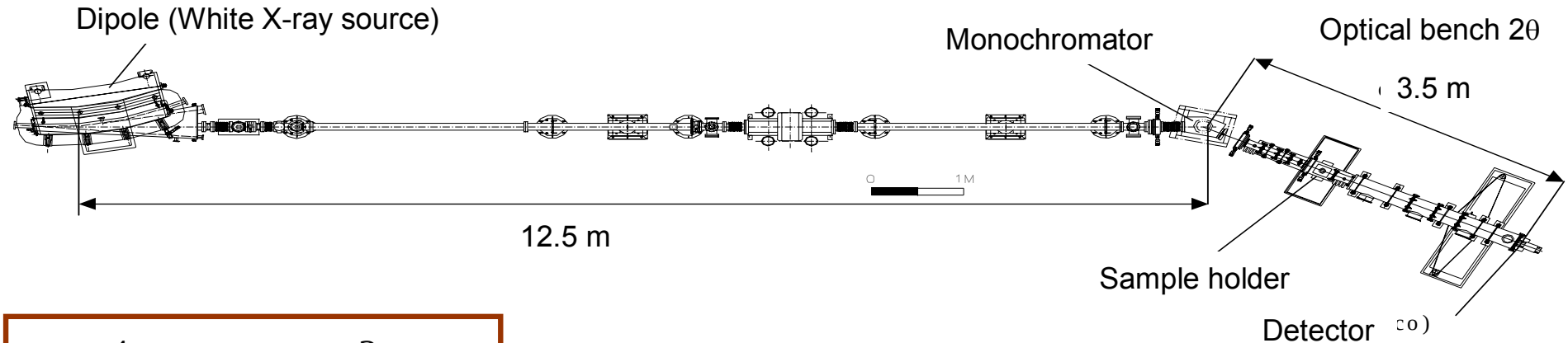

$$q = \frac{4\pi}{\lambda}\sin\left(\varepsilon/2\right) \cong \frac{2\pi}{\lambda}\varepsilon$$

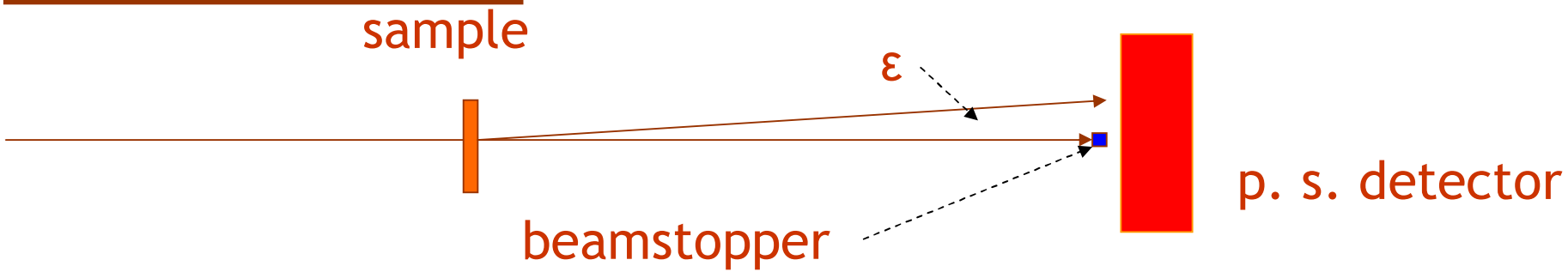

The shape of the proteins in solution. Folding-unfolding process. The envelope function

Solution of the phase problem

Dilute and monodisperse solutions

Ideality (high dilution) and monodispesity

$$I(q) = N\ I_1(q)$$

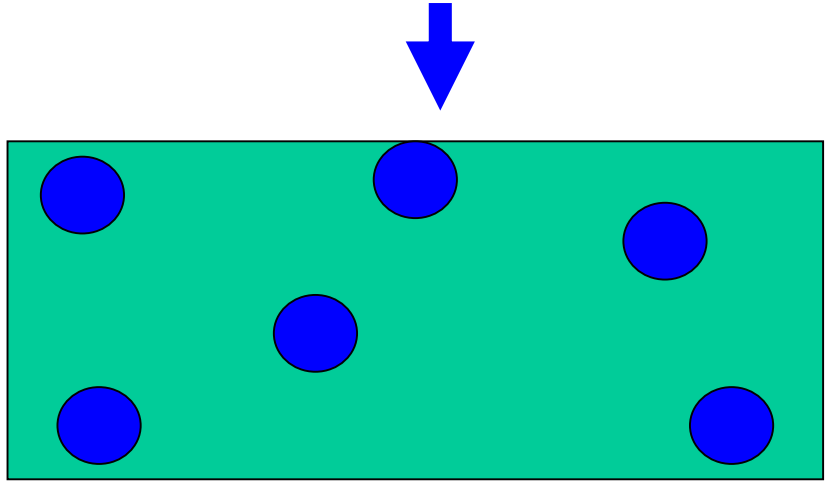

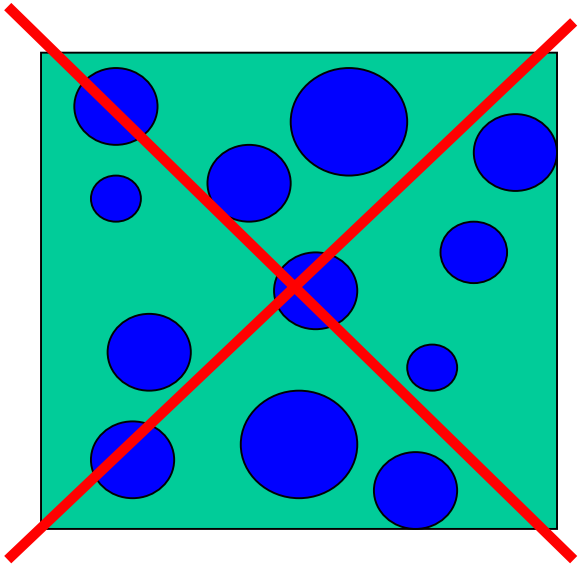

Small-angle scattering by a macroscopically isotropic material

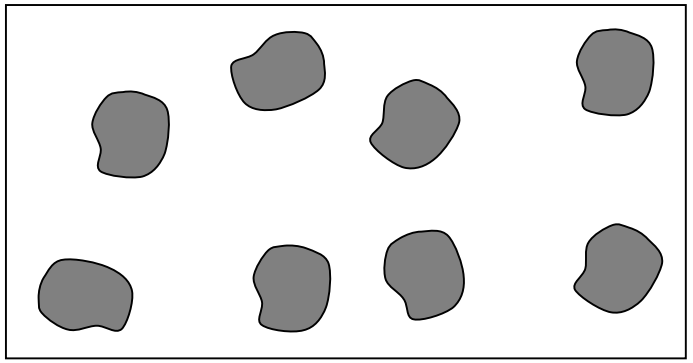

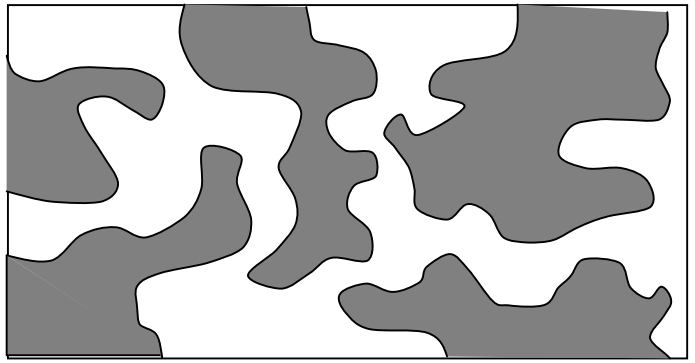

$$\left\langle e^{-i\vec{q}.\vec{r}} \right\rangle = \frac{\sin qr}{qr}$$

$$\gamma(r) = \frac{1}{8\pi^3 V I_e} \int_0^\infty 4\pi q^2 I(q) \frac{\sin q.r}{q.r} dq$$

$$\gamma(0) = \frac{1}{V} \int_V \Delta\rho(\vec{r}).\Delta\rho(\vec{r}).d\vec{r} = \overline{\Delta\rho(\vec{r})^2}$$

$$I(q) = I_e V \int_0^\infty 4\pi r^2 \gamma(r) \frac{\sin q.r}{q.r} dr$$

$$\gamma(0) = \frac{1}{8\pi^3 V I_e} Q$$

$$Q = \int_0^\infty 4\pi q^2 I(q) dq$$

Small-angle scattering of a dilute system of isolated nano-objects. General equations

The reduced correlation function for a single isolated object

$$I(q) = \sum_{i=1}^{N} I_1(\vec{q}) = N\left[\frac{1}{N}\sum_{i=1}^{N} I_1(\vec{q})\right] \qquad I(q) = N\left\langle I_1(\vec{q})\right\rangle$$

$$\gamma_0(r) = 1 - (S_1/4V_1)r \qquad \gamma_0(r) = \gamma(r)/\left[(V_1/V)(\rho_1 - \rho_2)^2\right]$$

$$\int_V 4\pi.r^2\gamma_0(r).dr = V_1$$

$$I_1(q) = I_e(\rho_1 - \rho_2)^2 V_1 \int_0^{D_{\max}} 4\pi r^2 \gamma_0(r)\frac{\sin q.r}{q.r}dr$$

$$I(0) = I_e N(\rho_1 - \rho_2)^2 V_1^2$$

$$V_1 = 8\pi^3 \frac{I(0)}{Q}$$

Asymptotic trend of the scattering intensity at small q. Guinier law
Dilute and monodispersed system (identical nano-objects)

$$I(q) = I_e N(\rho_1 - \rho_2)^2 V_1 \int_0^{D_{\max}} 4\pi r^2 \gamma_0(r) \frac{\sin qr}{qr} d\vec{r}$$

$$I(q) = I_e N(\rho_1 - \rho_2)^2 V_1 \int_0^{D_{\max}} 4\pi r^2 \gamma_0(r).(1 - \frac{q^2 r^2}{6})]dr \qquad (\sin qr/qr) = 1 - (q^2 r^2/6) + \ldots$$

$$I(q) = I_e N(\rho_1 - \rho_2)^2 V_1^2 \left[1 - \frac{q^2}{6}\frac{1}{V_1}\int_0^{D_{\max}} 4\pi r^2 \gamma_0(r) dr\right] = I_e N(\rho_1 - \rho_2)^2 V_1^2 \left[1 - \frac{q^2}{6} R_g^2\right]$$

$$R_g^2 = \frac{1}{V_1}\int_0^{D_{\max}} 4\pi r^2 \gamma_0(r) dr \qquad R_g = \left[\frac{1}{V}\int_V r^2 d\vec{r}\right]^{1/2} = \overline{r^2} \qquad R_g = \left\{\frac{\int_V \rho(\vec{r}).r^2.d\vec{r}}{\int_V \rho(\vec{r}).d\vec{r}}\right\}^{1/2}$$

$$I(q) = I_e N(\rho_1 - \rho_2)^2 V_1^2 . e^{-\frac{R_g^2 q^2}{3}}$$

Guinier law

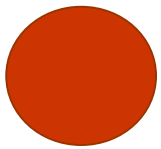

$$R_g = \sqrt{3/5}R$$

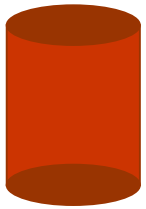

$$R_g = \sqrt{(D^2/8) + (H^2)/12}$$

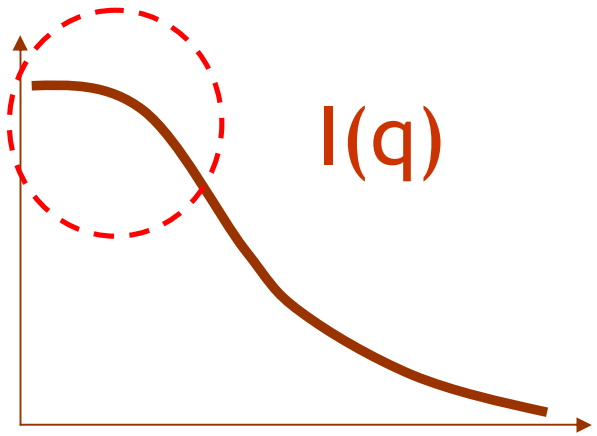

$$I(q) = I_e N(\rho_1 - \rho_2)^2 V_1^2 . e^{-\frac{R_g^2 q^2}{3}}$$

$q \rightarrow 0$

Ln I versus q^2 (Guinier plot)

$R_g = (3.\alpha)^{1/2}$

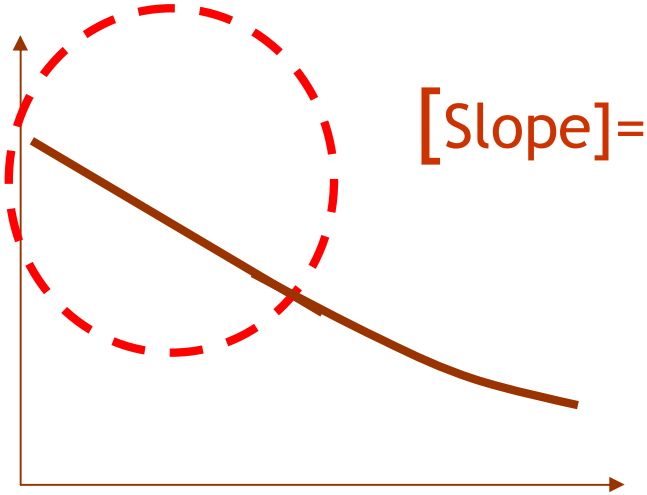

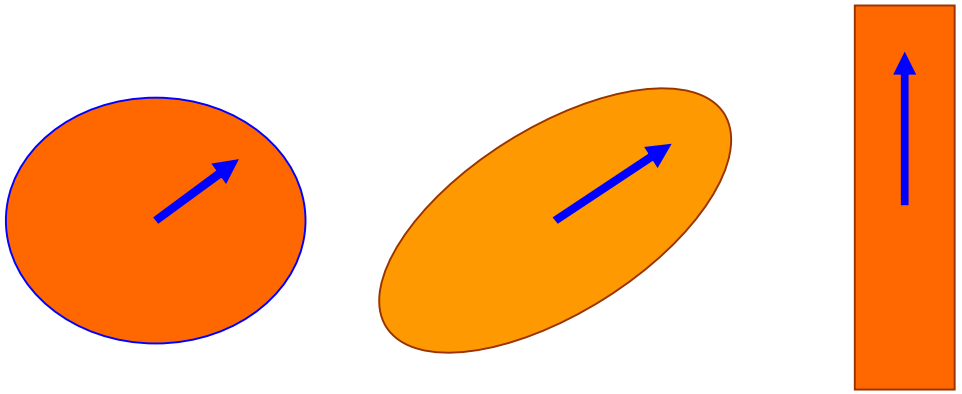

SAXS by an arbitrary two electron density model
The integral of the scattering intensity in reciprocal space
Asymptotic behavior of scattering curves at high q. Porod's law

$$\gamma(r) = \varphi_1\varphi_2\left(\rho_1 - \rho_2\right)^2\gamma_0(r) \qquad I(q) = I_e V\varphi_1\varphi_2\left(\rho_1 - \rho_2\right)^2\int_0^\infty 4\pi r^2\gamma_0(r)\frac{\sin q.r}{q.r}dr$$

$$\gamma_0(r) = 1 - \frac{S/V}{4\varphi_1\varphi_2}r + \ldots \qquad \gamma_0(r) = \frac{1}{8\pi^3 V I_e\varphi_1\varphi_2\left(\rho_1 - \rho_2\right)^2}\int_{Vq} 4\pi q^2 I(q)\frac{\sin q.r}{qr}dq$$

$$Q = \int_0^\infty 4\pi q^2 I(q)dq$$

$$Q = 8\pi^3 V I_e\varphi_1\varphi_2\left(\rho_1 - \rho_2\right)^2$$

Porod' s law ($q \to \infty$)

$$I(q) = \frac{2\pi I_e\left(\rho_1 - \rho_2\right)^2.S}{q^4}$$

For dilute and monodisperse systems

$$Q = I_e.N.V_1.8\pi^3\left(\rho_1 - \rho_2\right)^2$$

$$\frac{S_1}{V_1} = 4\pi^2\frac{[Iq^4]_{q\to\infty}}{Q}$$

$$I_1(q) = 4\pi \int_0^\infty p(r) \frac{\sin qr}{qr} dr$$

$$p(r) = \frac{r^2}{2\pi^2} \int_0^\infty q^2 I(q) \frac{\sin qr}{qr} .dq$$

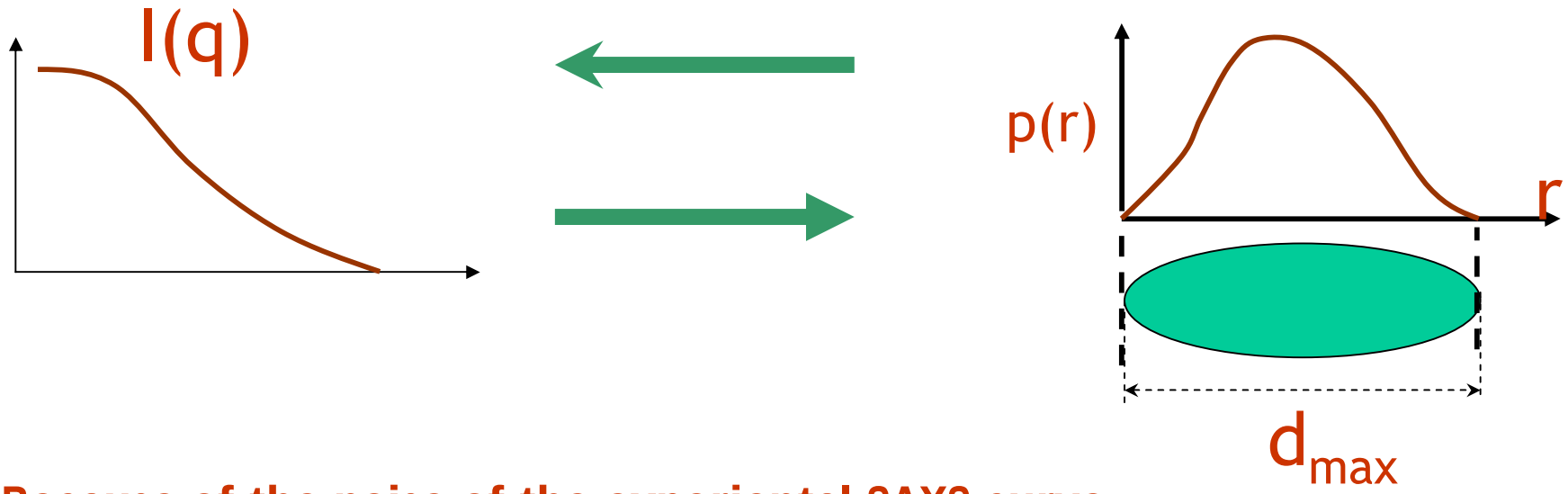

Because of the noise of the experiental SAXS curve and the limited q range of SAXS measurements, the mathematical problem for deriving p(r) from I(q) is "ill-defined". It can be solved using different programs such as GNOM (Svergun)

Structure parameters and function than can be directly derived from SAXS curves of proteins in solution

- R_g radius of gyration
- V_1 : volume
- S_1 : external surface
- p(r) : distance distribution function
- d_{max} maximum diameter

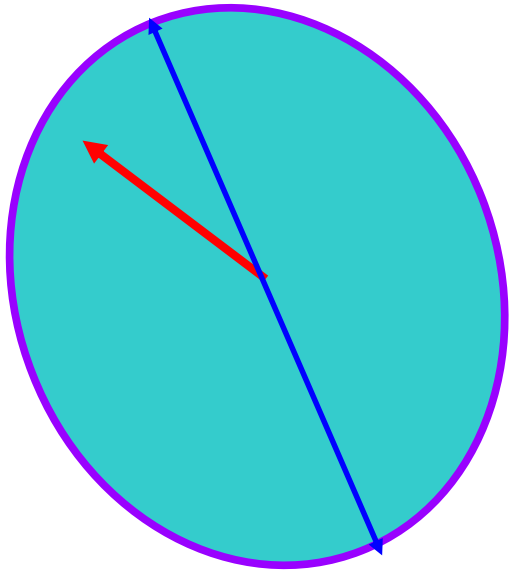

Detailed shape ???

Practical solution of the phase problem in SAXS studies

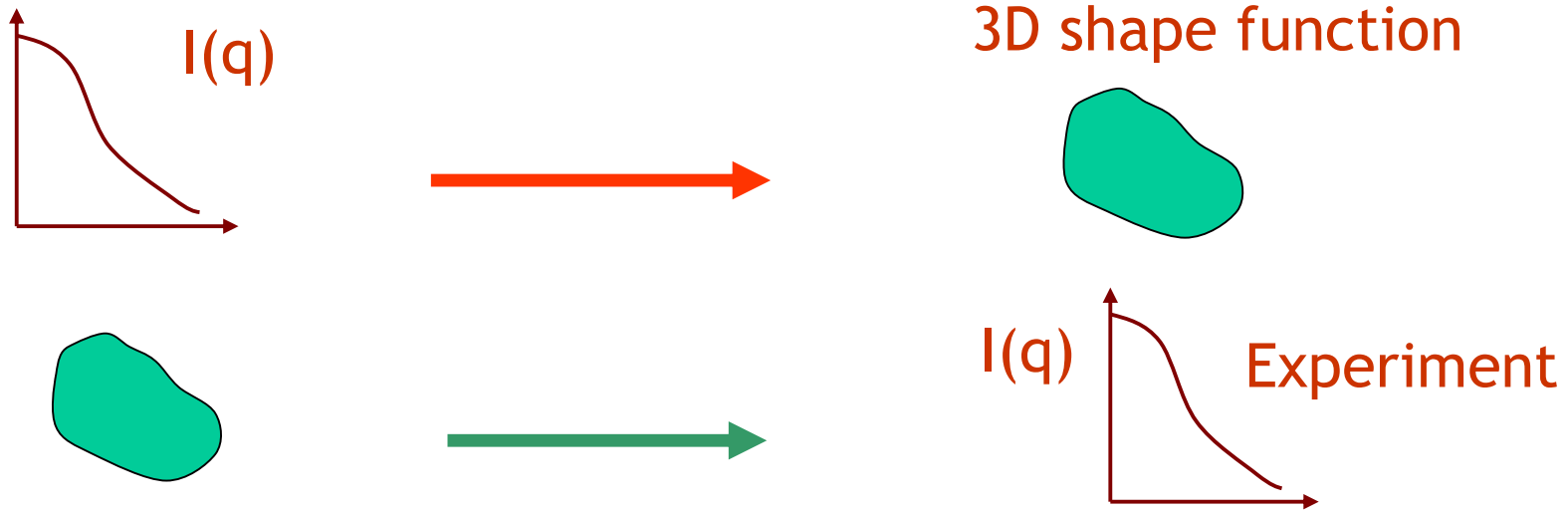

1) Guessing an initial shape. From the knowledge of Dmax, an initial spherical shape with R=dmax/2 is proposed.
2) Calculation of the scattering intensity I(q) for the initial (homogeneous) spherical protein.
3) Comparison with the experimental curve. Calculation of the Discrepancy parameter Chi.
4) A number of modifications of the shape leading to the minimum value of Chi.

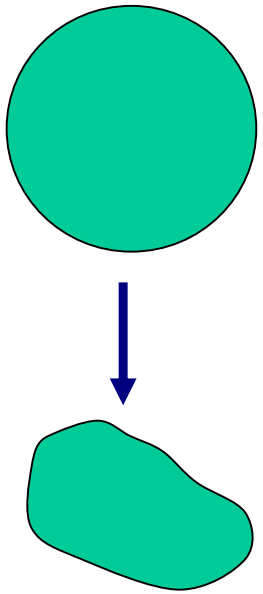

Proteins in solution

- Restauration of structural models *ab initio* using only results of small-angle scattering experiments
- Characterization of proteins in solution using SAXS and (high resolution) crystallographic data obtained by single crystal XRD
- Example of application: Phosphoenolpyruvate carboxykinase (PEPCK)

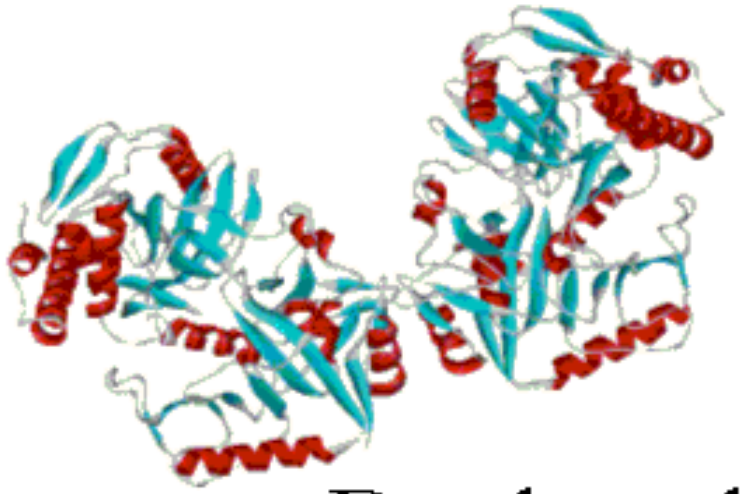

Bead models

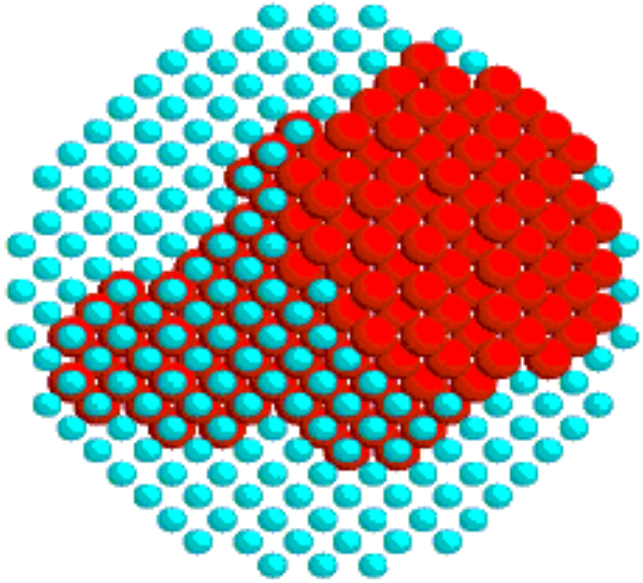

Position(j) = X(j) = 1 or 0

- $M \approx (D_{max}/r_0)^3 \approx 10^3 >> N_s$ parameters, too many for conventional minimization
- No unique shape restoration unless constrained
- Able to describe complex shapes

Chacón, P. *et al.* (1998) *Biophys. J.* **74,** 2760-2775.

Svergun, D.I. (1999) *Biophys. J.* **76,** 2879-2886

Ab initio program DAMMIN

Using simulated annealing, finds a compact dummy atoms configuration X that fits the scattering data by minimizing

$$f(X) = \chi^2[I_{\exp}(s), I(s, X)] + \alpha P(X)$$

where χ is the discrepancy between the experimental and calculated curves, *P(X)* is the penalty to ensure compactness and connectivity, $\alpha > 0$ its weight.

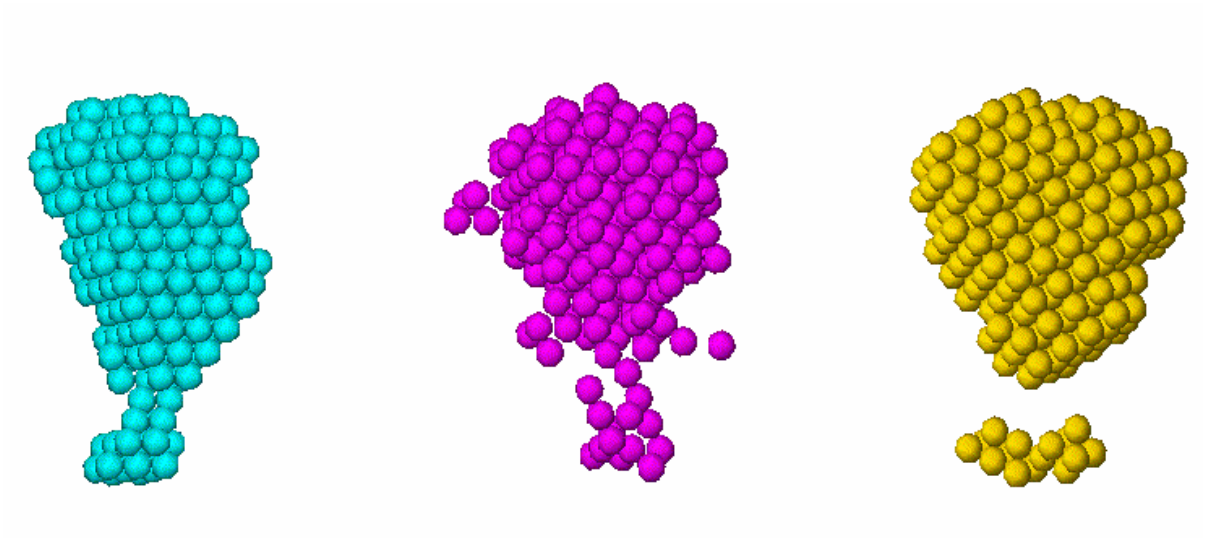

compact

loose

disconnected

Local and global search

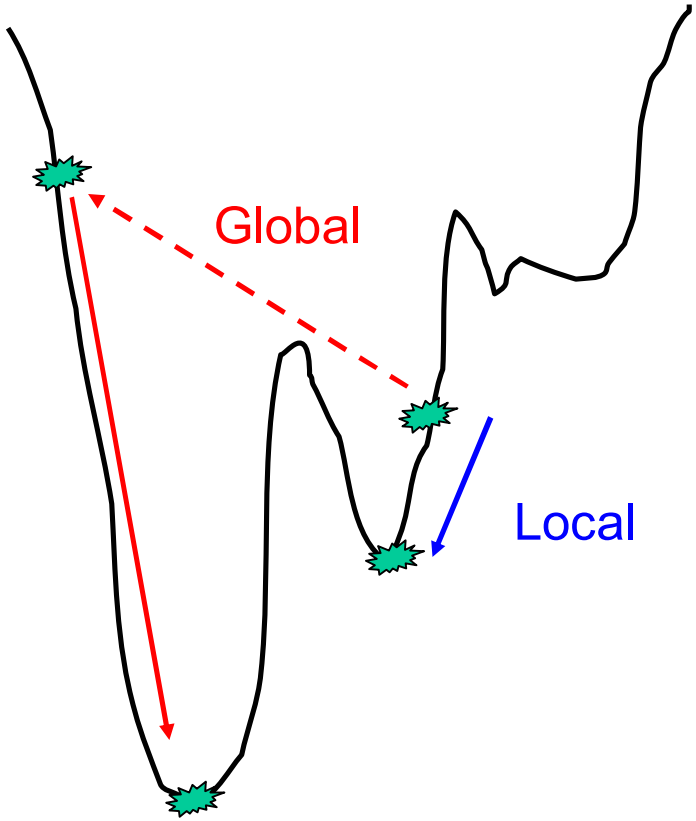

- Local search always goes to a better point and can thus be trapped in a local minimum
- To avoid local minima, global search must be able go to a worse point

S1 shape reconstruction

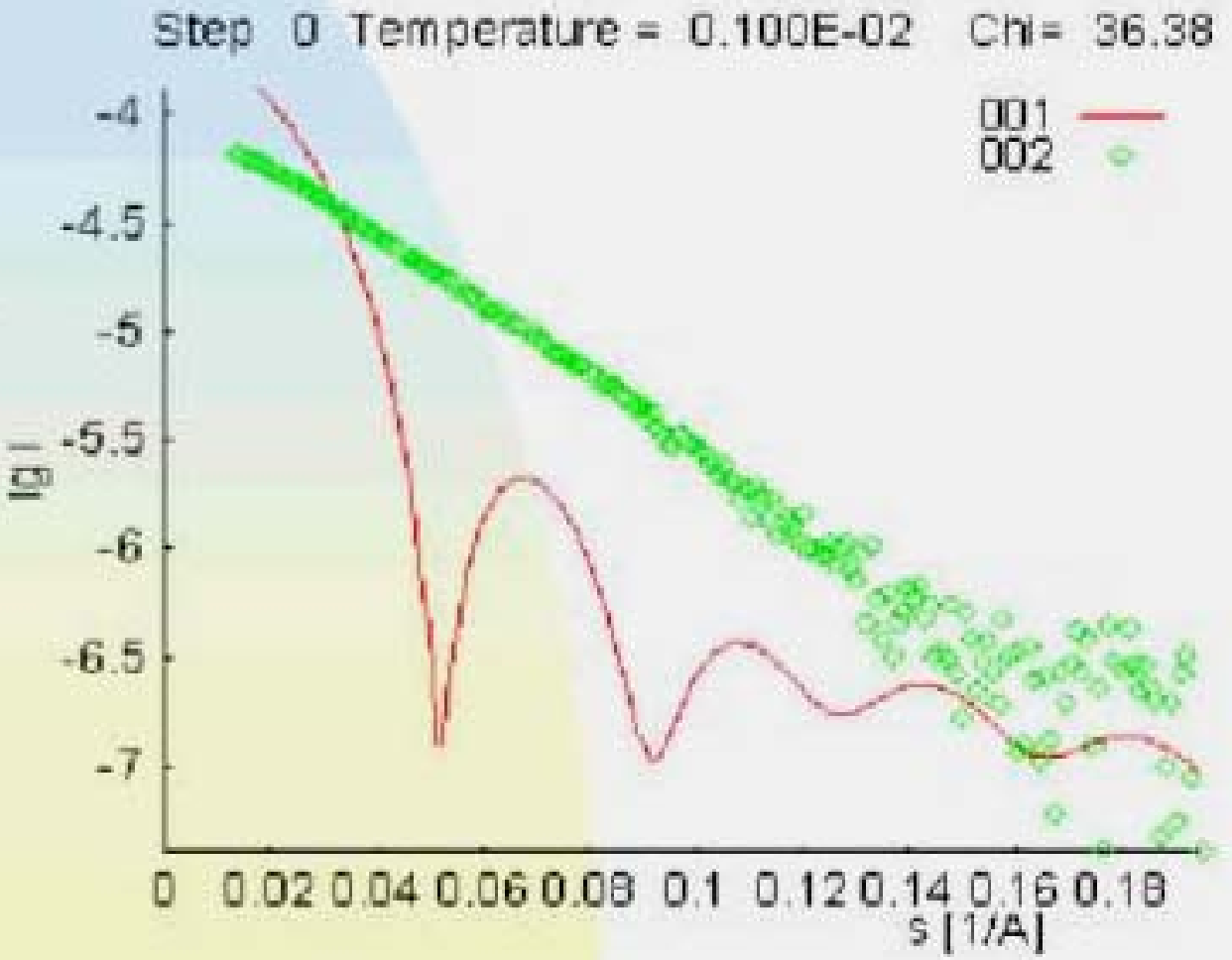

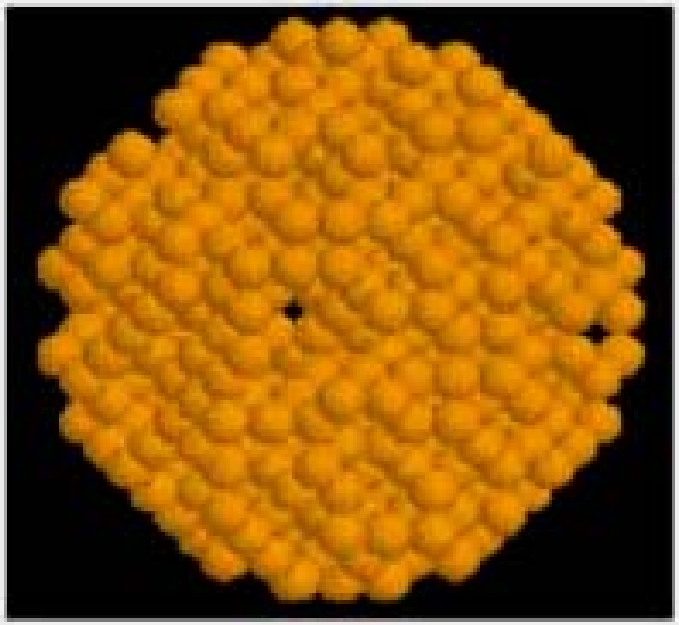

S1 shapes restored by *SASHA and DAMMIN*

Red: atomic model

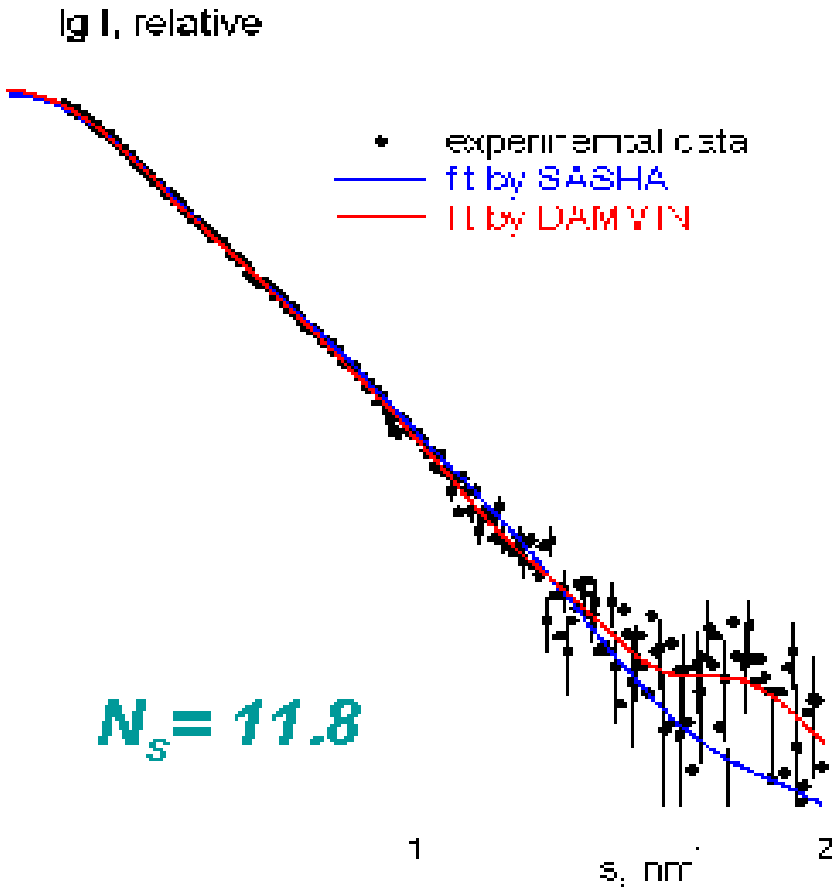

$N_s = 11.8$

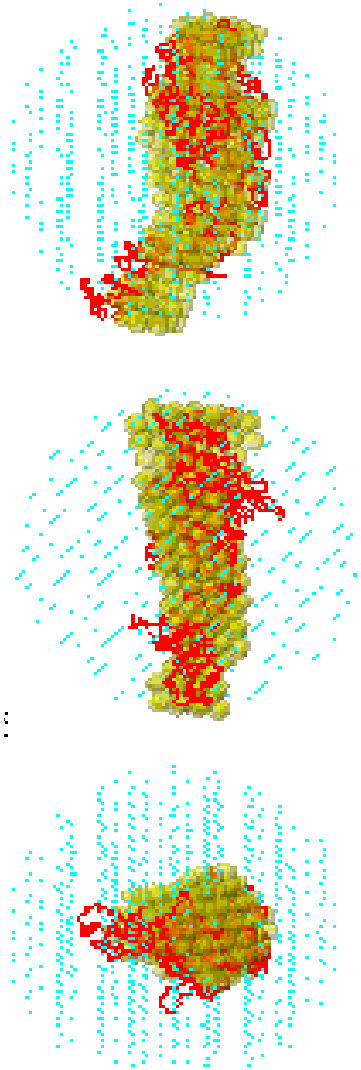

Number of parameters:

M=2729

Some examples of application of SAXS to the study of proteins

Crystal Structure of the Dimeric Phosphoenolpyruvate Carboxykinase (PEPCK) from Trypanosoma cruzi at 2 Å Resolution

Stefano Trapani, Jutta Linss, Samuel Goldenberg, Hannes Fischer, Aldo F. Craievich and Glaucius Oliva

J. Mol. Biol. (2001) 313, 1059-1072

Structure of the dimeric phosphoenolpyruvate carboxykinase (PEPCK) from trypanosoma cruzi

. Trapani, J. Linss, S. Goldenberg, H. Fischer, A. F. Craievich and G. Oliva, J. Mol. Biol. (2001) 313, 1059-1072

SAXS study of PEPCK in solution

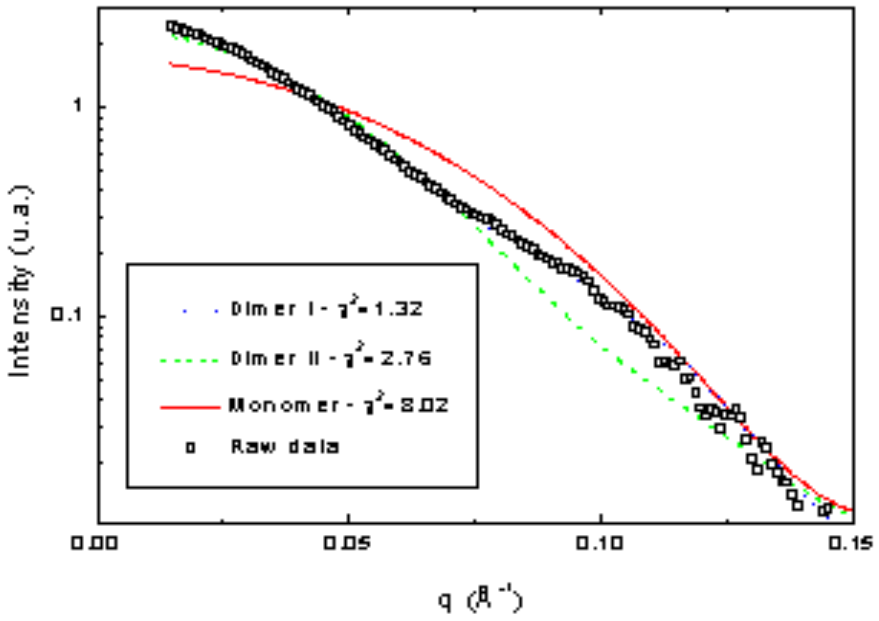

XRD studies of PEPCK protein single crystals > Structure of the unit cell

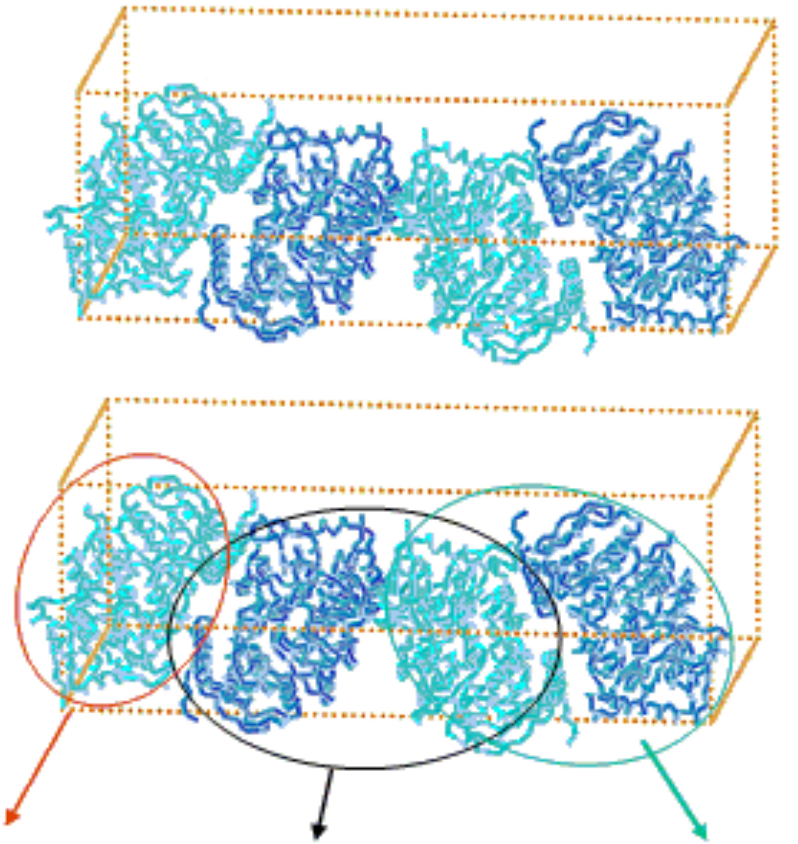

Three hypothesis:

Low resolution structure obtained from SAXS results by using Dammin

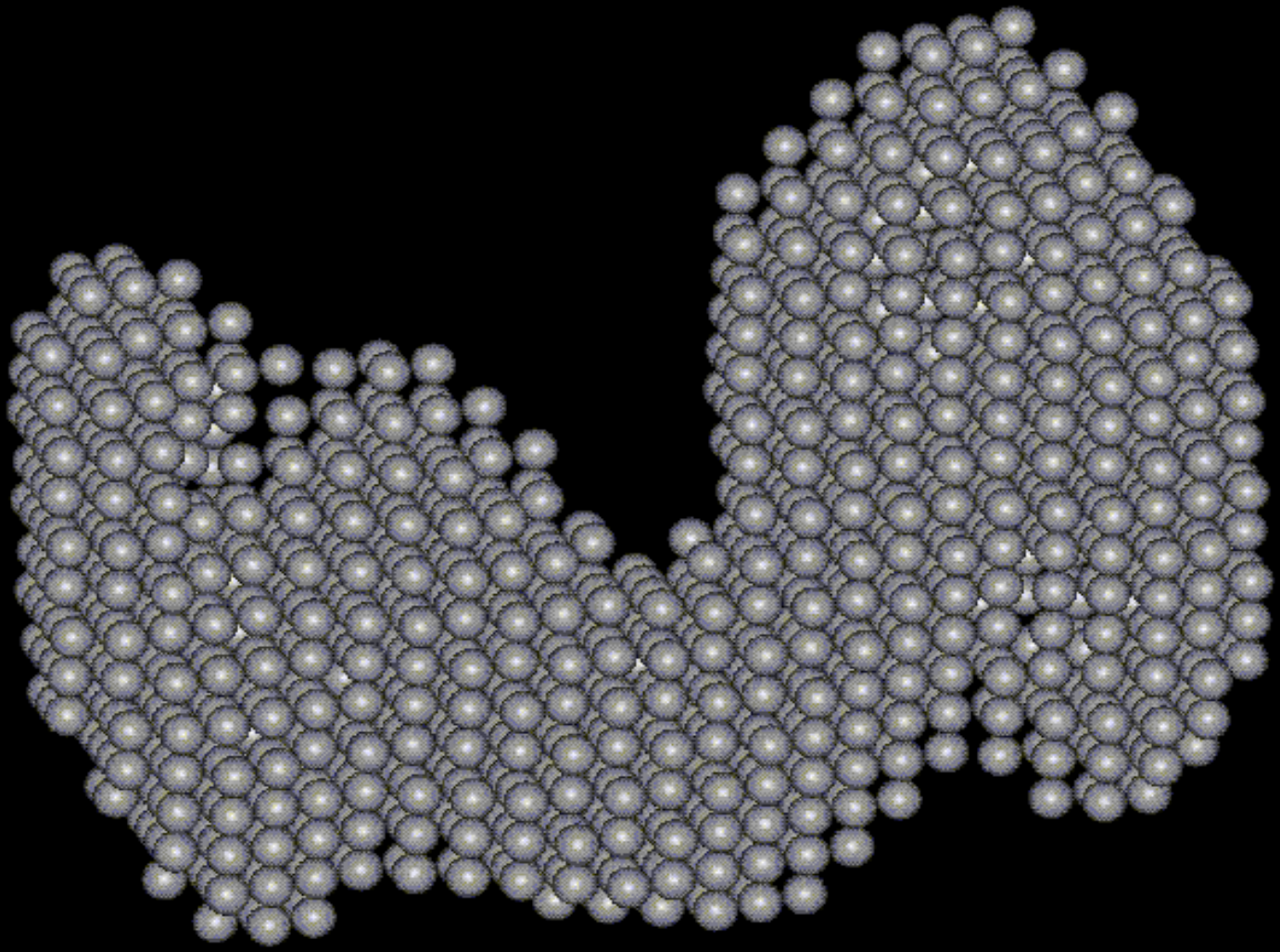

Domain motions and quaternary packing of phosphofructokinase-2 from Escherichia coli studied by small angle X-ray scattering and homology modeling

R. Cabrera, H. Fischer, S. Trapani, A.F. Craievich, R.C. Garrat, V. Guixe and J. Babul. Journal of Biological Chemistry. 278, 12913-9 (2003).

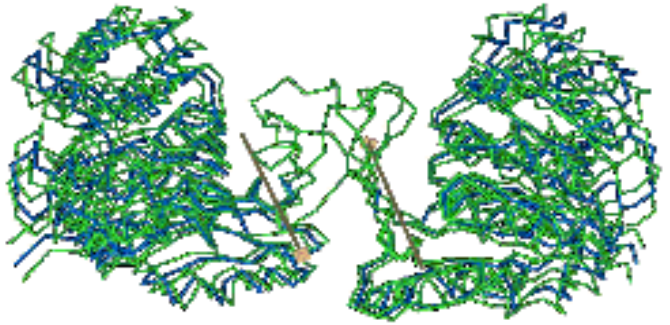

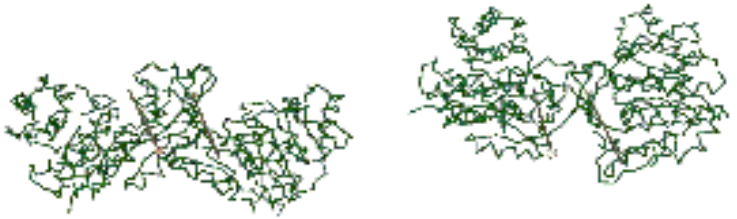

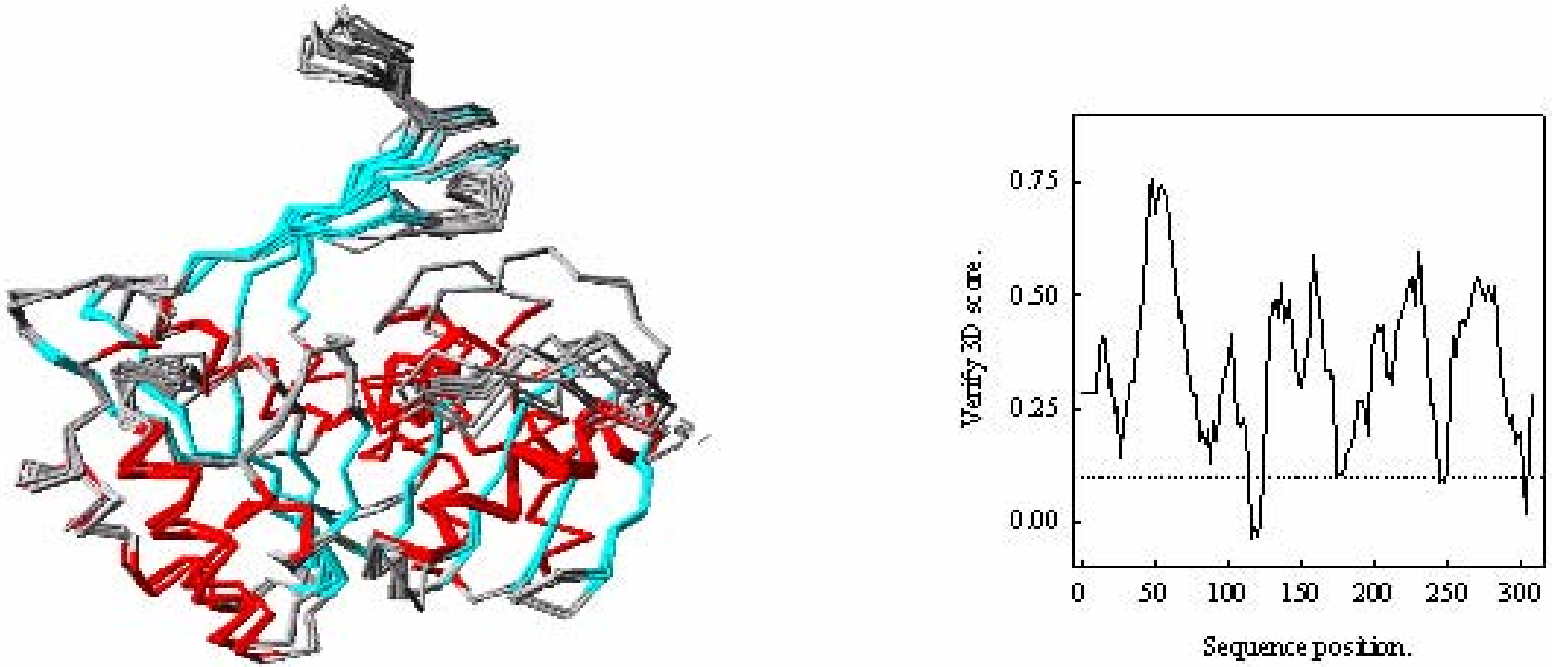

Figure 1. Homollogy modelling of Pfk-2.
(A) Superposition of ten CA trace models of monomeric Pfk-2 generated by MODELLER. Red color indicates a-helix, this color indicates b-strands, otherwise backbone is colored gray. (B) Mean 3D score profile for models shown in (A).

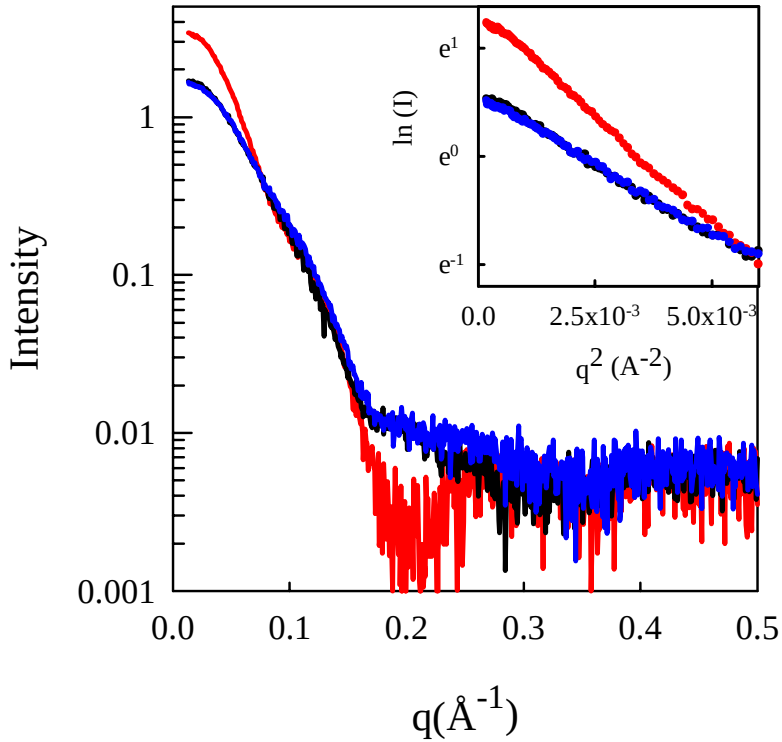

Solution scattering curves of Pfk-2 without and with ligands. In absence of ligands (black curve), with saturating Fru-6-P (blue curve) and in presence of excess of MgATP (red curve). Inset shows Guinier plot giving values shown in table I.

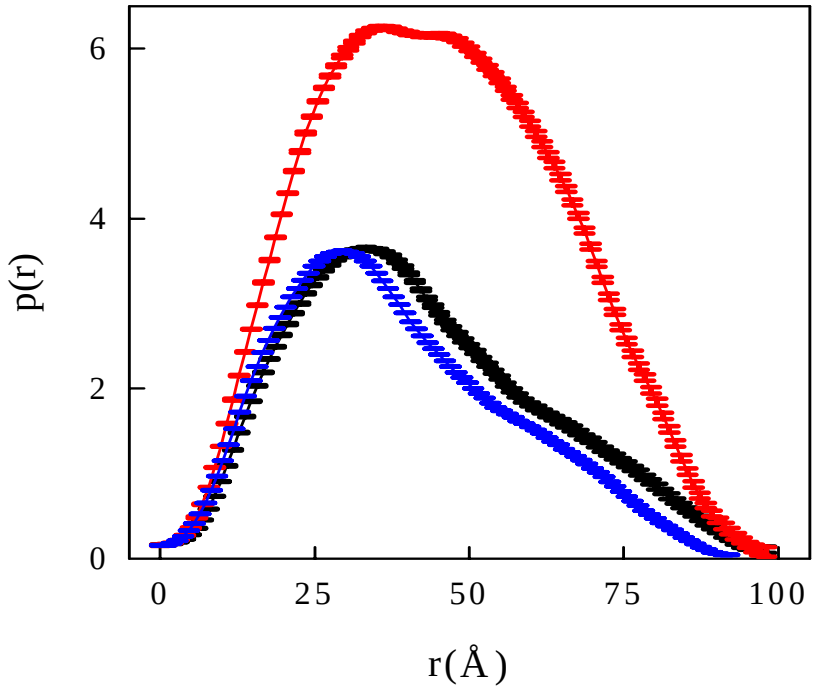

Distance distribution function for Pfk-2 without and with ligands. Curves were calculated using GNOM program from SAXS data of Pfk-2 in absence of ligands (black curve), Pfk-2 in presence of excess Fru-6-P (blue curve) and excess of MgATP (red curve).

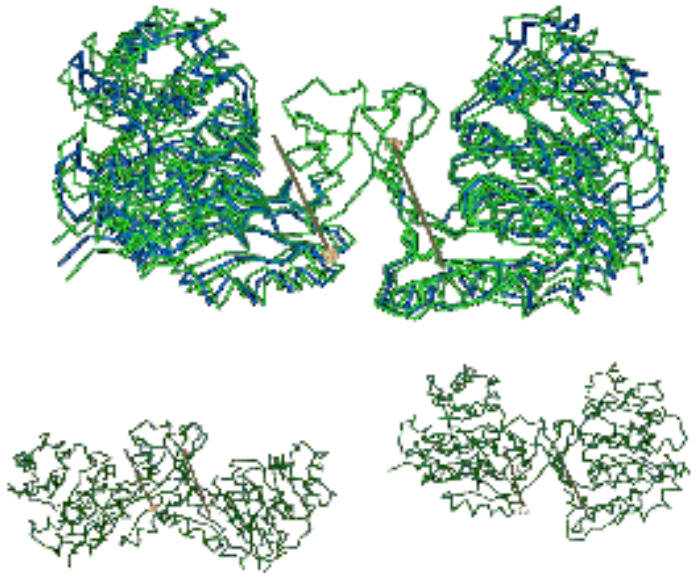

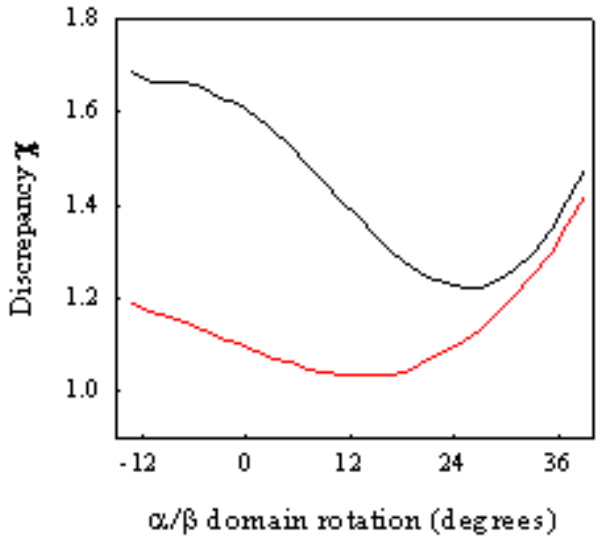

Modelling Fru-6-P induced conformational changes.
Top, trace drawings of Pfk-2 homology model showing rigid rotations around the calculated rotation axes (parallel brown arrows); bottom, left and right, trace drawing for the most open (40˚) and most closed (-20˚) structures, respectively. **(Right side)** Discrepancy between the experimental data and the simulated scattering from the models.

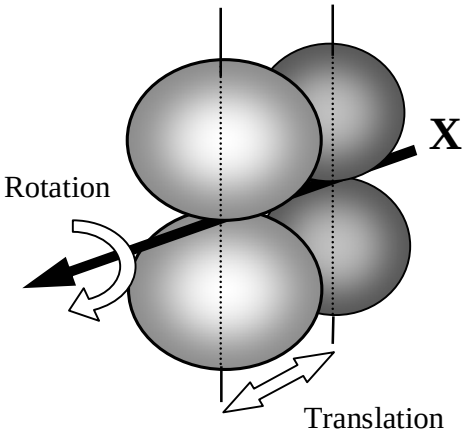

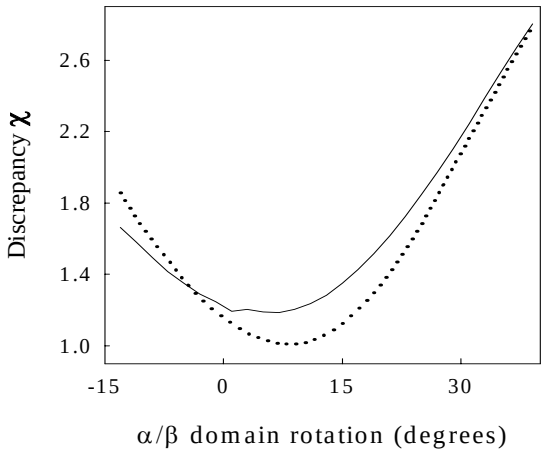

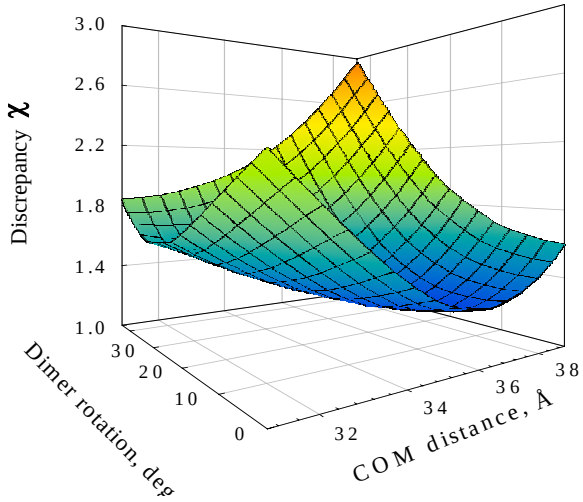

Modelling quarternary packing in tetramer (with Mg-ATP).

(A). Schematic diagram showing X simmetry axis (black arrow) along which, rotations and translations were made.

(B). Chi value of the better adjust of rotation and COM distance with SAXS data for every degree of a/b domain openness. Curves for tetramer-I (solid line) and tetramer-II (dotted line).

(C). Plot showing Chi value for every combination of rotation and distance modelled for 7 deg domain openness dimer.

References

-“Structural insights into the beta-mannosidase from T-reesei obtained by synchrotron small-angle X-ray solution scattering enhanced by X-ray crystallography”. R. Aparicio, H. Fischer, D.J. Scott, K.H.G. Verschueren, A.A. Kulminskaya, E.V. Eneiskaya, K.N. Neustroev, A.F. Craievich, A.M. Golubev and I. Polikarpov. Biochemistry-US 41 (30): 9370-5 (2002).

-“Crystal structure of the dimeric phosphoenolpyruvate carboxykinase (PEPCK) from trypanosoma cruzi at 2 A resolution”. S. Trapani, J. Linss , S. Goldenberg, H. Fischer, A.F. Craievich and G. Oliva. Journal of Molecular Biology 313, (5) 1059-72 (2001).

-“Domain motions and quaternary packing of phosphofructokinase-2 from Escherichia coli studied by small angle X-ray scattering and homology modeling”. R. Cabrera, H. Fischer, S. Trapani, A.F. Craievich, R.C. Garrat, V. Guixe and J. Babul. Journal of Biological Chemistry. 278, 12913-9 (2003).

--“Low resolution structures of the retinoid X receptor DNA-binding and ligand-binding domains revealed by synchrotron X-ray solution scattering”. H. Fischer, S.M.G. Dias, M.A.M. Santos, A.C. Alves, N. Zanchin, A. F. Craievich, J. W. Apriletti, J. D. Baxter, P. Webb, F.A.R. Neves, R.C.J. Ribeiro, and I. Polikarpov. Journal of Biological Chemistry. 278, 16030-8 (2003).

-“Free human mitochondrial GrpE is a symmetric dimer in solution”. J. C. Borges, H. Fischer, A.F. Craievich, L.D. Hansen, C. H. Ramos. Journal of Biological Chemistry. 278, 35337-44 (2003).

The Brazilian synchrotron light laboratory - LNLS) - Campinas

www.lnls.br


Brazilian Synchrotron Light Laboratory
LNLS
Laboratório Nacional de Luz Síncrotron
LNLS

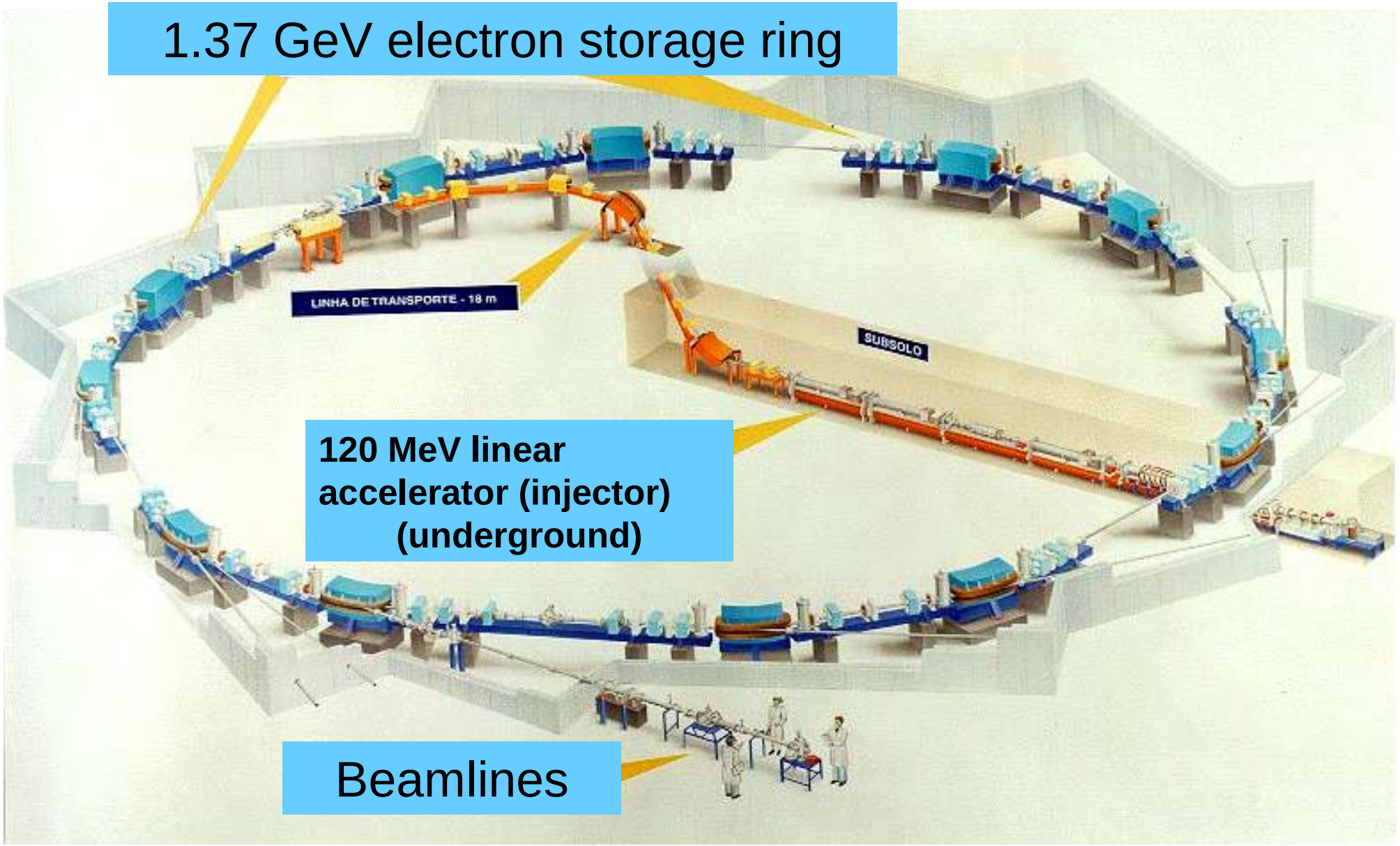
1.37 GeV electron storage ring
LINHA DE TRANSPORTE - 18 m
SUBSOLO
120 MeV linear accelerator (injector) (underground)
Beamlines

Construction and commisioning period: 10 anos

June 1987: Starting

December 1989: 50 MeV LINAC operation

Agust 1995: Starting the installation of the beamlines

July 1997: Opening to the external users

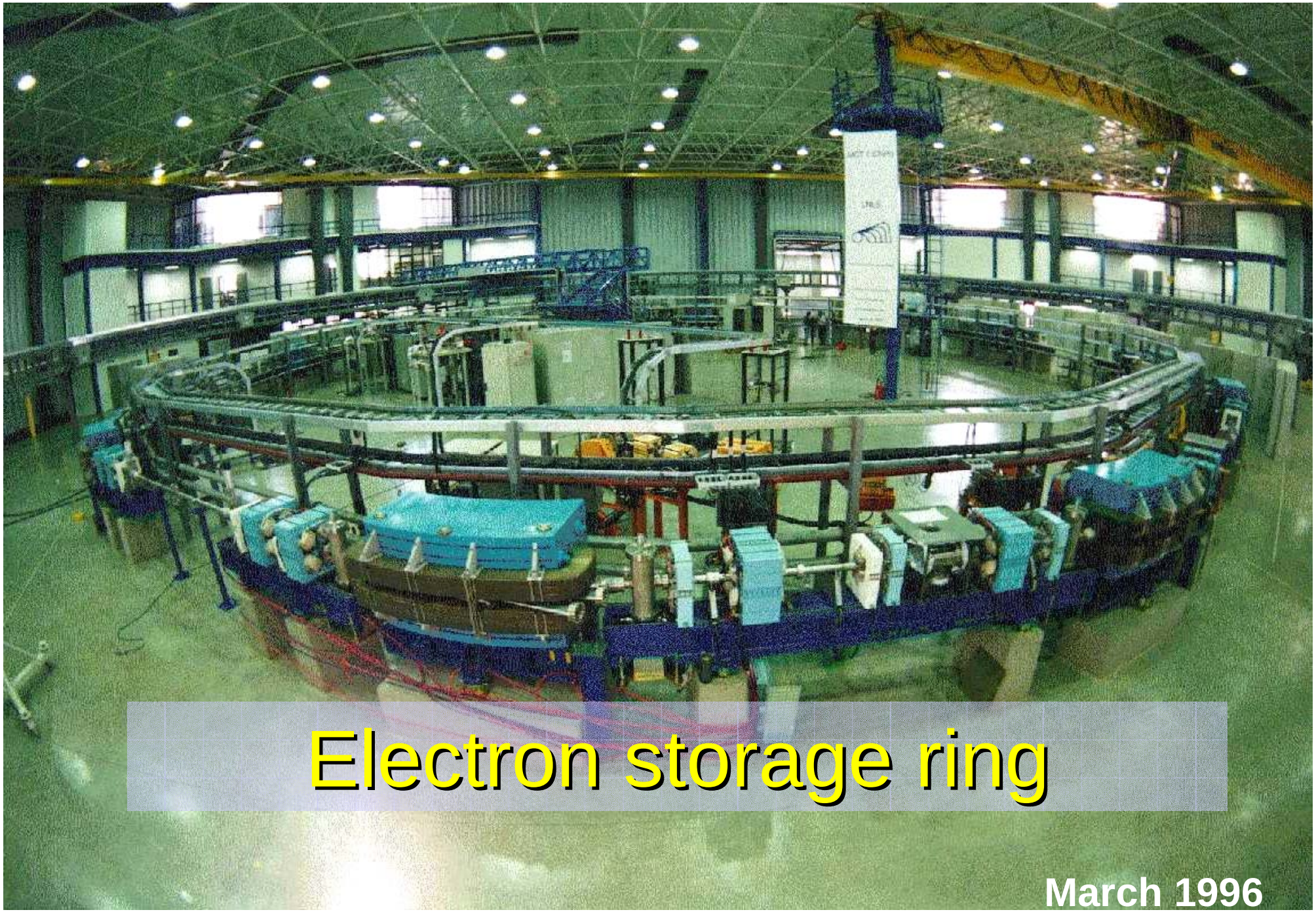
Electron storage ring
March 1996

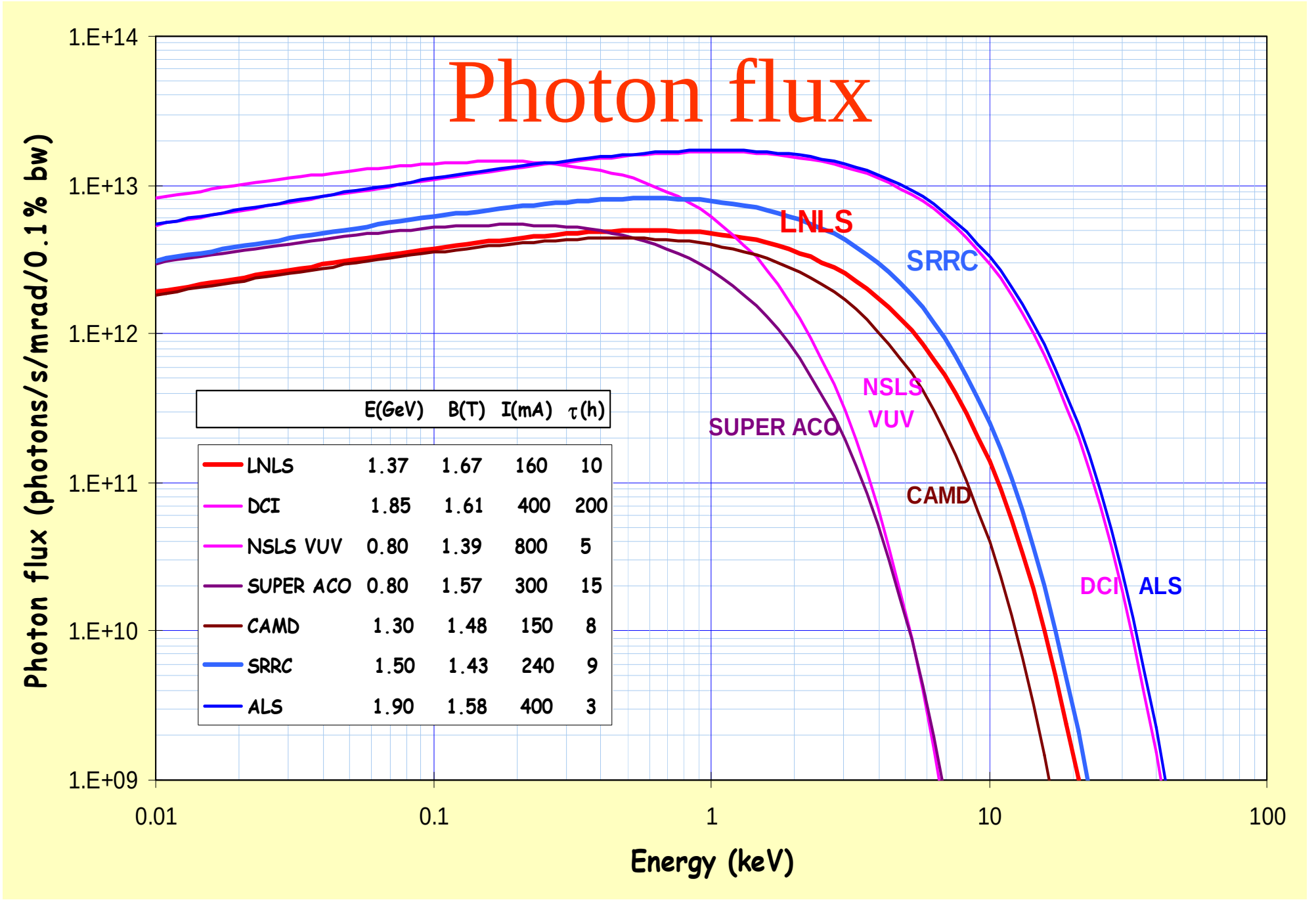
Photon flux
Photon flux (photons/s/mrad/0.1% bw)
1.E+14
1.E+13
1.E+12
1.E+11
1.E+10
1.E+09
0.01
0.1
1
10
100
Energy (keV)
LNLS
SRRC
NSLS VUV
SUPER ACO
CAMD
DCI
ALS
E(GeV) B(T) I(mA) τ(h)
LNLS 1.37 1.67 160 10
DCI 1.85 1.61 400 200
NSLS VUV 0.80 1.39 800 5
SUPER ACO 0.80 1.57 300 15
CAMD 1.30 1.48 150 8
SRRC 1.50 1.43 240 9
ALS 1.90 1.58 400 3

Operation parameters

	Specified	Achieved		
		Jul-97	Dec/98	
Energy	1.15	1.37	1.37	GeV
Current	100	75	170	mA
Lifetime (@100 mA)	7	2.2	16	hours


APPLICATIONS:
Materials Science
Biology
Chemistry
Physics
Microfabrication
Environmental science
...

SAXS beamline

Special instrumentation for the beamlines

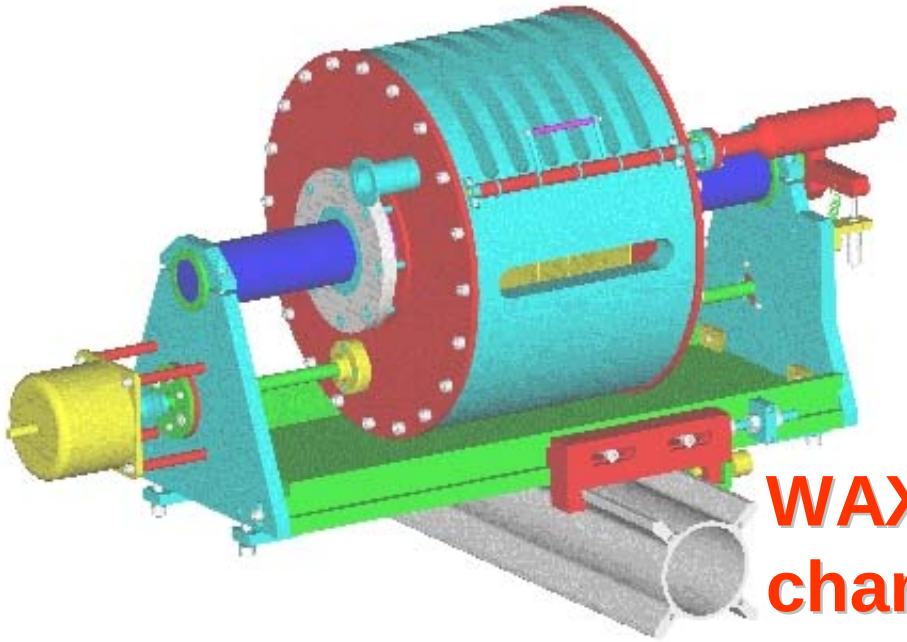

WAXS/SAXS chamber

Capillary microfocusing

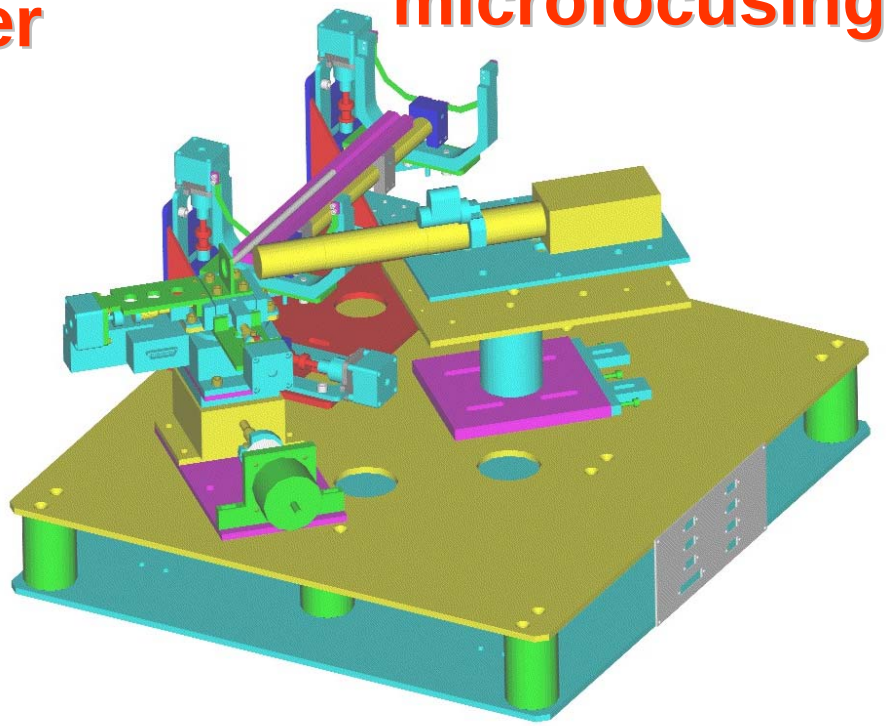

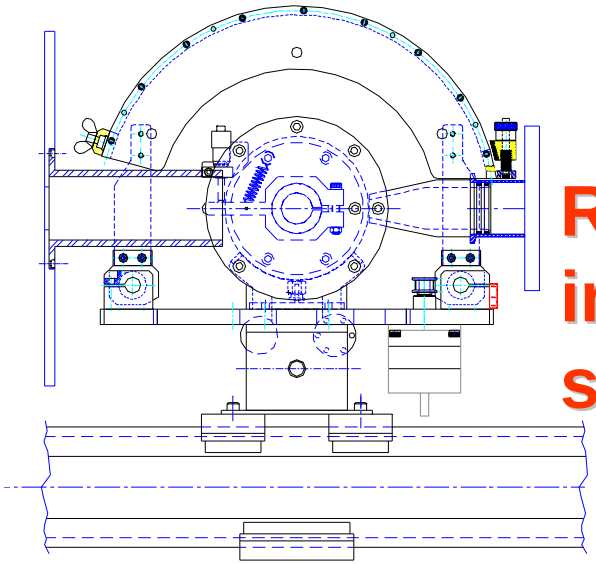

Reactor for in-situ x-ray studies

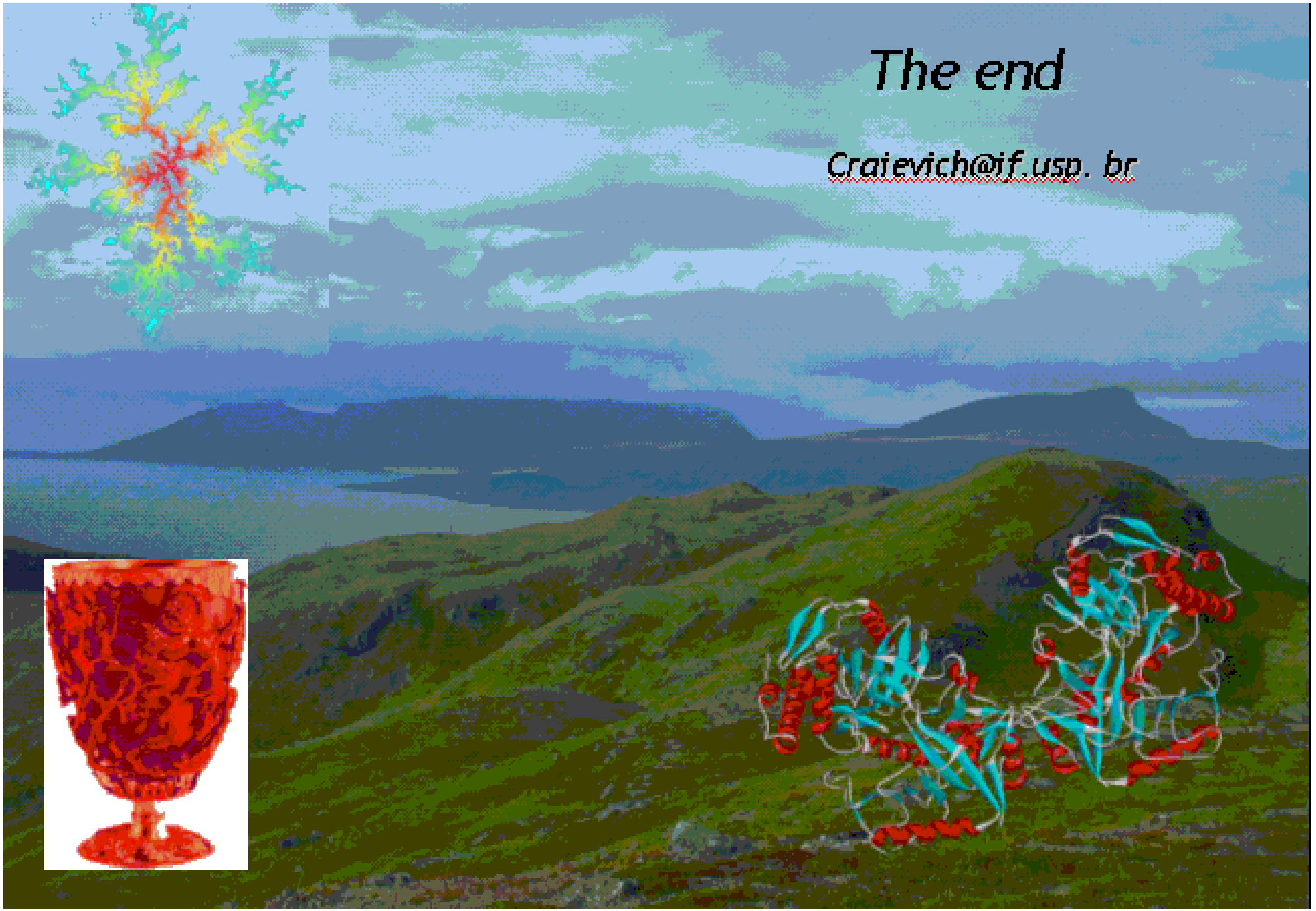
The end
Craievich@if.usp. br